RESEARCH ARTICLE

Aerosol characteristics and aerosol radiative forcing over Maitri, Antarctica

H. Gadhavi and A. Jayaraman*

Physical Research Laboratory, Ahmedabad 380 009, India

During the 20th Indian Antarctic expedition conducted in January–February 2001, a detailed study on the aerosol spectral optical depth, mass concentration and size-distribution along with columnar ozone and water-vapour concentrations was made from the Indian station, Maitri (70.77°S, 11.73°E). A low aerosol optical depth of about 0.03 at 400 nm wavelength and a dry aerosol mass concentration of about 7 µg/m^3 for the PM_{10} particles are found for this anthropogenically least-affected continent on the earth. The aerosol size-distribution reveals that about 63% of the total aerosol mass comes from particles of size greater than 1 µm, which are of mainly natural origin. Average columnar ozone and total precipitable water-vapour content during the observation period were found to be 271.6 DU and 0.147 cm respectively, and the observed day-to-day variations are explained using air back-trajectory analysis. Estimation of aerosol radiative forcing over Maitri reveals a positive forcing of 0.95 W/m^2 at the top of the atmosphere and –0.83 W/m^2 at the surface. Using model calculations, it is shown that these forcing values can have large annual variation both in magnitude and sign due to variation in the sun–earth geometry, typical of a polar region, even if we assume a constant aerosol amount throughout the year.

AEROSOLS are tiny particles of different chemical composition, suspended in air for a duration ranging from a few hours to a few days. Aerosols can impact the earth's weather and climate by altering the earth's radiation budget mainly through scattering and absorbing the solar radiation and to a lesser extent, by absorbing the outgoing terrestrial long-wave radiation. The high spatial and temporal variations of the aerosol concentration and their physical and chemical properties make it difficult to assess quantitatively, the exact impact on climate. However, field experiments such as the Indian Ocean Experiment[1] (INDOEX), the Tropospheric Aerosol Radiative Forcing Experiment[2] and Aerosol Characterization Experiment[3] help to get the necessary data over a specific region and season, which are useful for model impact analysis. Over continents the amount of aerosol is generally large compared to the interior ocean region because the particles are produced both due to natural processes such as wind-blown dust, accidental forest-fires, etc. as well as due to man-made activities such as industries, vehicular traffic and biomass-burning. Over the ocean it is mainly the sea-salt particles produced by breaking of air bubbles by surface winds and to a lesser extent, sulphate particles produced from dimethyl sulphide emitted by phytoplanktons. Several recent studies[1,4–6] conducted over the ocean surrounding peninsular India as well as over some selected locations in the Indian mainland show high aerosol radiative forcing, which is a measure of the net reduction or increase in the amount of surface-reaching or outgoing radiation flux due to total columnar aerosol burden. There are also results[1,7] showing that radiation is absorbed within the atmosphere by particles such as soot. However, the Antarctic region is unique. In the absence of any major local aerosol source, the air is generally pristine and is only influenced by the long-range transport of sub-micron-size particles and gaseous pollutants from other parts of the globe. The objective of the present study is to examine the characteristics of the aerosol particles found in the Antarctic and to estimate their radiative forcing. In the last few decades there has been a considerable increase in anthropogenic activities both in developed and developing nations, which is responsible for an overall increase in the aerosol burden around the globe. Aerosol and radiative-forcing studies over sites such as Antarctica will help in estimating the background-level aerosol forcing over a pristine site, which could be compared with results obtained over polluted regions. Also, such a study helps in establishing a database that could be used in future for studying the long-term impact of continuous human activities in increasing the background-level aerosol concentration. Factors like high surface albedo and unique solar insolation cycle over Antarctica also make the study an interesting one. The present field study made at the permanent Indian Antarctic Station, Maitri (70.77°S, 11.73°E) during the 20th Indian Antarctic Expedition provides the continuity to aerosol optical-depth measurements made over Antarctica by other groups[8–11]. Also, by including results on aerosol size-distribution and radiative-transfer analysis, additional information is provided which is of use to global climate-change study.

*For correspondence. (e-mail: jraman@prl.ernet.in)

Experiment

The 20th Indian Antarctic expedition was launched from Goa on 28 December 2000. The team arrived at Maitri on 14 January 2001. Aerosol studies were carried out from 18 January to 23 February 2001. A hand-held sun-photometer was used to measure the aerosol optical depth and a quartz crystal microbalance (QCM) cascade impactor was used to measure the surface-level aerosol mass-concentration and size-distribution. Measurements of columnar ozone and water-vapour were carried out using Microtops-II.

Aerosol optical depth

Aerosol optical depth (AOD) is a measure of the attenuation of direct solar radiation that occurred while passing through the atmosphere containing aerosols. It critically depends upon the amount, size-distribution and chemical composition of aerosols. AOD information can readily be used to estimate the aerosol radiative forcing. A hand-held sunphotometer, built in-house at the Physical Research Laboratory (PRL), Ahmedabad has been used for AOD measurements. Optical interference filters are used to select the spectrum of interest from near-UV to near-IR region. The measurement is based on the principle that $I(\lambda) = I_0(\lambda)e^{-m\tau}$, where I and I_0 are the instantaneous solar irradiances at the surface and top of the atmosphere, m is relative airmass and τ is the total optical depth. $\tau(\lambda) = \tau_a(\lambda) + \tau_{ray}(\lambda) + \tau_{ma}(\lambda)$, where τ_a is the aerosol optical depth, τ_{ray} is optical depth due to Rayleigh scattering by air molecules and τ_{ma} is the optical depth due to molecular absorption. I is the quantity which is measured using the sun photometer, while other quantities are to be calculated. I_0 is estimated using the standard Langley plot technique[12] in which the logarithm of the photometer output is plotted against airmass and extrapolated to 'zero' airmass. The airmass, m is a function of solar zenith angle and is calculated using astronomical formulae and corrected for atmospheric refraction as well as the earth's curvature effect[13]. τ_{ray} is estimated for the polar summer atmosphere using the Rayleigh scattering cross-section calculated following Nicolet[14]. τ_{ray} is also corrected for the actual atmospheric-pressure variation observed over the site, which varied between 967.1 and 994 mbar. This corresponds to a variation of about 0.01 in the short wave optical depth and less at higher wavelengths. Prior to and after the expedition, the interference filters were calibrated in-house for changes, if any, in the filter-transmission characteristics and are included in the computation of the optical depth due to molecular gases. Important gases responsible for absorption in the wavelength region used in the present study are ozone, water-vapour and oxygen. Optical depth due to these gases is calculated using the SBDART[15] (Santa Barbara Discrete ordinate Atmospheric Radiative Transfer) model which is based on the low-resolution band models developed for the LOWTRAN 7 atmospheric transmission code. Total columnar concentration of ozone and water-vapour was measured using Microtops-II, and used to obtain the optical depths due to ozone and water-vapour absorptions. For oxygen, summer-time polar model atmosphere values are used. The estimated optical-depth values due to Rayleigh scattering and molecular absorptions for the mean condition are given in Table 1. Measurements were made at five wavelength regions centred around 400, 497, 668, 875 and 1058 nm with a typical bandwith of 10 nm at approximately 15 min interval, whenever clouds are not obscuring the sun or are not in the vicinity of about 30 degrees around the sun. A total of about 220 measurements were made for each wavelength region during the campaign period.

Aerosol mass concentration

A QCM, California Measurements Inc, USA is used to measure the mass size-distribution of aerosols at the surface level. Details of the instrument and its working principle can be found in Wallace and Chuan[16]. The instrument has 10 stages with each stage sensitive to a specific size range of particles. The radii at which the collection efficiency is maximum are 8.64, 4.26, 2.24, 1.08, 0.55, 0.29, 0.16, 0.07 and 0.03 μm respectively, for the stages 2 to 10 and the respective full width at half maximum changes from about 7 to 0.03 μm. The instrument was kept around 225 m away in a wooden hut, in a northward direction from the main station to avoid contamination from any localized sources such as power generator, kitchen, etc. Air sample was drawn at a height of 2 m from the ground level. The sampling arrangement is configured vertically such that there is negligible loss of particles within the sampling tube. About 3 to 4 measurements were taken every day. Prior to the starting of the measurement, drift if any, in the crystal frequency was checked each day, and was found to be negligible and random. No special correction has been done for this variation. Error in the measurement of total mass is estimated to be within 25%, found earlier by simultaneously

Table 1. Columnar optical depth due to Rayleigh scattering and molecular absorption at various wavelengths for average Antarctic conditions

Central wavelength of filter (nm)	τ_{ray}	τ_{O_3}	τ_{H_2O}	$\tau_{(O_2 + N_2)}$
400	0.3778	$\sim 10^{-5}$	0	0.0002
497	0.1517	0.0090	0	0.0003
668	0.0464	0.0135	0.0008	0.0016
875	0.0153	0	0.0024	0
1058	0.0077	0	0.0077	0.0083

operating this instrument with others like Anderson impactor[4].

Columnar O_3 and H_2O concentrations

Microtops-II sun-photometer, manufactured by Solar Light Co, USA is used for direct measurements of the column concentrations of ozone and water-vapour. The instrument measures direct solar radiation intensity at five spectral bands, viz. 300, 305.5, 312.5, 940 and 1020 nm. The first three UV channel data are used for the estimation of the total columnar concentration of ozone, expressed in Dobson Unit (DU), which is the equivalent thickness of pure ozone layer at standard pressure and temperature. The total precipitable column water-vapour concentration is calculated from the radiation measurements at 940 nm (having water-absorption peak) and 1020 nm (no absorption by water). The accuracy of the ozone and water-vapour measurements is better than 2%. More details of the instrument and measurement accuracy can be found in Morys *et al*.[17].

Meteorological conditions

Routine meteorological observations were made at the site. Additional data necessary for calculation of air back-trajectory analysis, etc. were obtained from Air Resource Laboratory (ARL) and NOAA–CIRES Climate Diagnostics Center, USA. The daily mean air temperature at Maitri during the campaign period was in the range of 0 to −10°C, with an average value of −3°C. A decreasing trend in daily mean temperature is observed from January to February, with cloudy days recording lower temperature than the mean trend. The relative humidity (RH) is found to be around 78 ± 7%, with a decreasing trend from January to February. Decreasing trends observed at both temperature and RH are indicative of the air becoming drier, typical of the transition from summer to winter season. The average surface-level wind speed was 7.1 m/s, but was highly variable and often reaching values of 12 m/s and above. However, no systematic trend in wind speed was observed during the campaign period. It should be noted that Maitri is located at the edge of the Antarctic continent and hence experiences wind from both ocean and inland, intermittently. This altering airmass has an important effect on the aerosol, ozone and water-vapour content over Maitri, as discussed in the following section.

Results and discussions

Daily variation in the mean AOD for the campaign period is shown in Figure 1, for two selected wavelengths of 400 and 1058 nm. Except for the two high values recorded on 18 and 19 January, during the remaining days the values were in the range 0.01 to 0.1 for all wavelengths. High values of AOD and high day-to-day variations are seen in the extreme wavelengths of 400 and 1058 nm compared to the intermittent region. Figure 2 shows the average AOD spectrum obtained for the whole period. Vertical bars over the datapoints represent the standard deviation for that day. The high values recorded on 18 and 19 January are not included for the estimation of the average spectrum. The AOD value at 400 nm is the maximum compared to those at longer wavelengths, with a mean value of 0.036 ± 0.018 and also exhibiting larger daily variability. The average AOD spectrum shows distinctly two modes, one peaking at a lower wavelength of 400 nm or below and the other at a higher wavelength of 1058 nm or above. This kind of feature is typical of an optically clean region where the AOD at the visible wavelength region is the minimum. The higher AOD at lower wave-

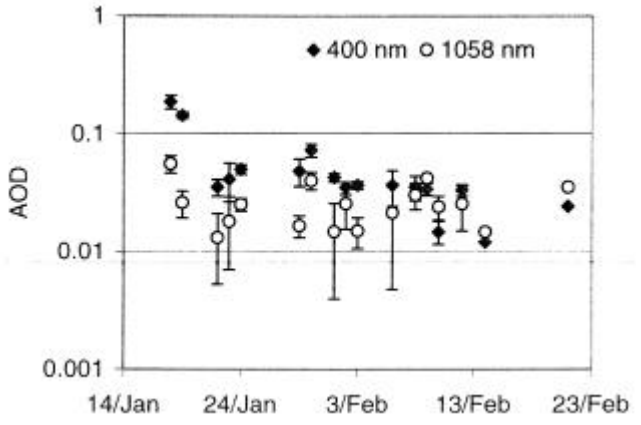

Figure 1. Day-to-day variation in daily mean aerosol optical depth (AOD) for two selected wavelengths measured over Maitri, Antarctic during January–February 2001 (top). AOD at other wavelengths also shows similar variation, but is not included to avoid clutter.

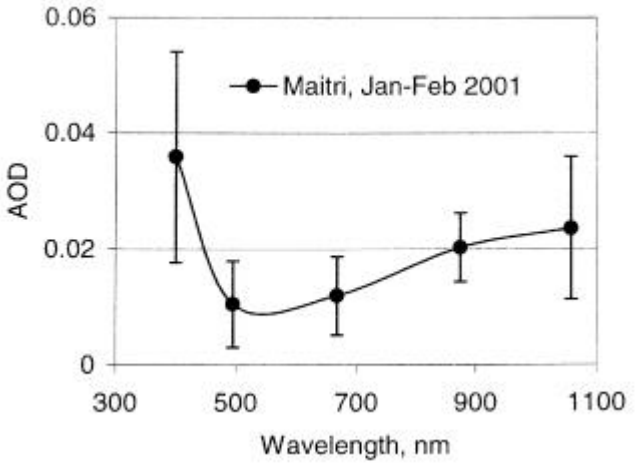

Figure 2. Mean AOD spectrum for the entire campaign period. The high AOD values obtained on 18 and 19 January (shown in Figure 1) are not included in the mean spectrum.

length is caused due to nucleation-mode particles, which are of sub-micron size. These particles are produced mainly *in situ* within the atmosphere by gas-to-particle conversion mechanism from precursor gases such as oxides of sulphur, nitrogen, etc. Owing to their small size, they have a higher residence time in the atmosphere compared to bigger particles. Also, the residence time increases with increasing altitude and in the free troposphere, these submicron particles have residence time of the order of a few weeks to a month, sufficient to sustain long-range inter-continent transport from their source origin to the polar region. Higher AOD values seen in the longer wavelength region is produced mainly by bigger size particles which are of local and natural origin and composed mainly of sea-salt particles from the ocean and dust debris from the underlying land. Shaw[8] has reported a value of 0.025 ± 0.010 for AOD over McMurdo station (77.85°S, 166.67°E) and 0.012 ± 0.005 over the South Pole for 500 nm. Herber *et al.*[9] report a value in the range of 0.02 to 0.025 at 1000 nm during the volcanically quiescent period at George Forster, which is near Maitri. Further, Herber *et al.*[9] found very little difference between the AOD values obtained at different stations for this wavelength. However, a higher AOD value of about 0.035 to 0.045 for 500 nm is reported[9] compared to those at stations George Forster, Mirny (67°S, 93°E), Molodeznaya (68°S, 46°E)[8].

The AOD values obtained over Maitri are lower than those obtained over other regions, including the clean Indian Ocean region. Figure 3 compares the mean AOD spectrum obtained over Maitri with those measured over other regions, obtained from similar sun-photometer observations made on-board ship cruises. In Figure 3, coastal India represents data collected along the west coast of India, Indian Ocean-North represents data collected over the Indian Ocean but north of the inter-tropical convergence zone (ITCZ), the region till which the influence of continental air from the north is felt, and Indian Ocean-South represents data collected south of the ITCZ, which has relatively less anthropogenic influence. The data shown are for the period January to March, similar to the present study, but are the average for the years 1996 to 1999. AOD at all wavelengths is the lowest over Antarctic and increases as we move towards the north, with the highest value obtained near coastal India. The interesting observation is that the increase in AOD from the pristine polar site to the polluted site is not uniform at all wavelengths, which is indicative of the change in columnar aerosol size-distribution and composition with latitude. For example, if one compares the Maitri data with the Indian Ocean-South data, though AOD values are high at all wavelengths over the Indian Ocean-South; the increase is more at wavelengths longer than 400 nm, indicating that the increase in the number of bigger particles is higher than that of the smaller particles. Smaller particles have longer residence time in the atmosphere and they are well mixed compared to coarse particles. Also, over the Indian Ocean the concentration of sea-salt particles is more compared to that over Maitri, and this contributes to the observed higher AOD at longer wavelengths. Between the AOD spectra over the Indian Ocean-South and the Indian Ocean-North, the major difference is in the lower-wavelength AOD indicating an increase in the concentration of smaller particles that are mainly transported from the continents towards the ocean. A more or less similar shape observed in the AOD spectra over Indian Ocean-North and coastal India shows that the aerosols are well mixed in these regions, except that the concentrations are higher in the coastal region.

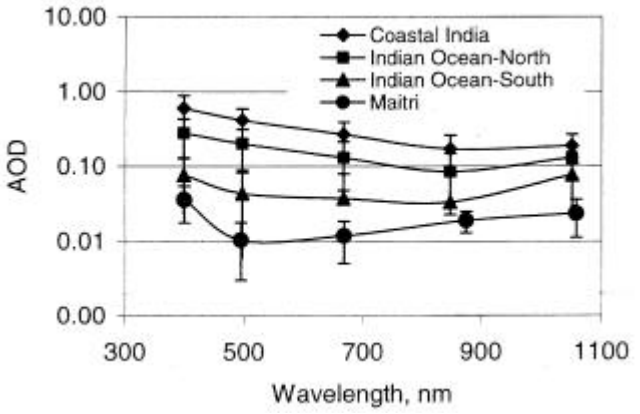

Figure 3. Comparison of mean AOD spectrum obtained over Maitri with those over other regions obtained during INDOEX cruises. Vertical bars represent ± 1 standard deviation of the mean. See text for explanation of the regions.

The average mass concentration of the ambient aerosol particles of size less than 10 μm (denoted as PM_{10} particles) at Maitri for the entire campaign period was 9.14 μg/m^3, with a standard deviation of 6.0 μg/m^3. The relatively large variation shows the extent of the day-to-day variability in the surface-level aerosol mass concentration over Maitri. Of the average total mass, the coarse particles having a size between 1 and 10 μm contribute 5.76 μg/m^3, which is 63% of the total (Figure 4). Similarly, the accumulation-mode particles having a size between 0.1 and 1 μm contribute 1.91 μg/m^3, which is 21%

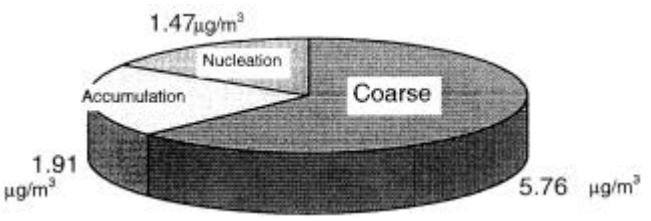

Figure 4. Average mass concentration of aerosol (PM_{10}) particles at Maitri during the campaign period was 9.14 μg/m^3, of which the coarse particles ($r > 1$ μm) contribute 5.76 (63%); the accumulation ($0.1 < r < 1$ μm) particles 1.91 (21%); and the nucleation ($r < 0.1$ μm) particles 1.47 (16%) μg/m^3.

of the total and the nucleation-mode particles having a size less than 0.1 μm contribute 1.47 μg/m^3, which is 16% of the total. The mass values shown are for the ambient measurements, meaning that they also contain water. If we correct for the water content, the dry (0% RH) PM_{10} aerosol mass becomes 6.97 μg/m^3 and at 50% RH, it becomes 7.87 μg/m^3. The major contribution to the total aerosol mass is from the coarse particles which have local origin, such as the sea-salt particles brought from the nearby ocean region as well as dust from the underlying surface. The aerosol mass concentration over Maitri is at least an order of magnitude low compared to those in other polluted parts of the world[18,19]. However, in comparison with other Antarctic stations such as McMurdo (77°51′S, 166°40′E), the Maitri value is high. Mazzera *et al*.[20] have found average PM_{10} in the range 3.21 to 4.81 μg/m^3 between the years 1995 and 1997, at two different locations over McMurdo station. Also over Maitri, an increasing trend is observed in the total mass value from January to the end of February. Increase in surface-level aerosol concentration as austral winter progresses has also been observed by other explorers (Hall and Wolff[21] and references therein). Hall and Wolff[21] have explained this seasonal increase by the effect of temperature on salinity of brine formed over newly-formed sea-ice surface. Richardson[22] has demonstrated through laboratory experiments that original sea-water salinity of 35‰ increases to 122‰ when temperature decreases from 0 to –8°C, and the surface brines formed are much better sources of sea-salt aerosol than sea-water. Over Maitri, the observed mass increase is however not monotonous, but with substantial decrease in values during 29 January to 2 February 2001, and on 6 February 2001. This is explained in terms of changing wind direction. Figure 5 shows wind stream line calculated from NCEP reanalysis data for 19 and 29 January 2001. On 29 January 2001, the wind is predominantly from the interior continent side compared to 19 January 2001. The inland continental air brings less aerosols to the measurement site than the wind from the ocean side, which remains the main source of aerosols over Antarctica.

In spite of the pristine atmosphere, large day-to-day variations in both the aerosol parameters as well as the column concentrations of ozone and water-vapour are recorded over Maitri. Though the ozone and water-vapour measurements were made to correct the AOD for the estimation of the radiative forcing over Maitri, which is the main objective of the present study, because of the large variations observed in the column ozone and water-vapour, it is interesting to present the results here. Figure 6 shows the daily average values of the measured integrated vertical columnar ozone and water-vapour concentrations, and the vertical bar over datapoints are standard deviation for that day. During the period from 3 to 11 February 2001, an episodic decrease in the ozone concentration by about 40 DU was observed from the normal background value of about 285 DU. Comparison of this observed decrease with TOMS[23] satellite data revealed that the decrease was localized mainly over the Maitri region. Atmospheric dynamics plays a major role in controlling the ozone concentration over this region, located at the edge of the polar

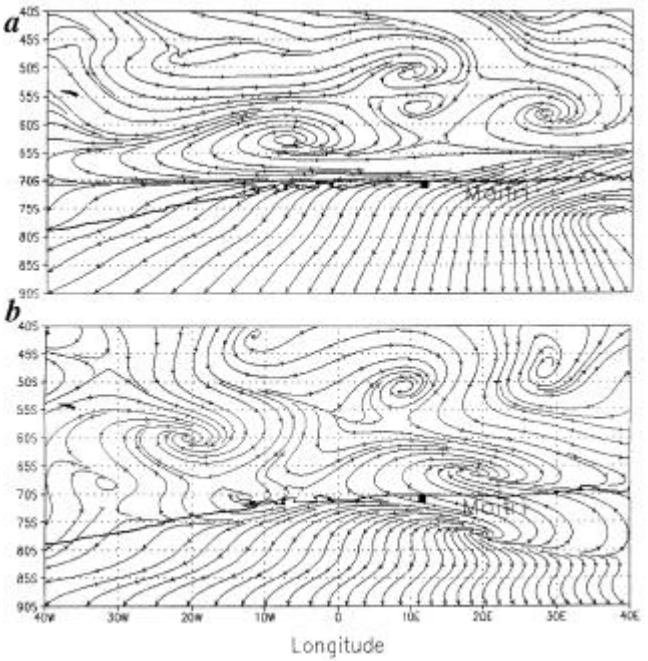

Figure 5. Wind stream line over Maitri on (***a***) 19 January 2001 and (***b***) 29 January 2001. Marker shows the position of Maitri.

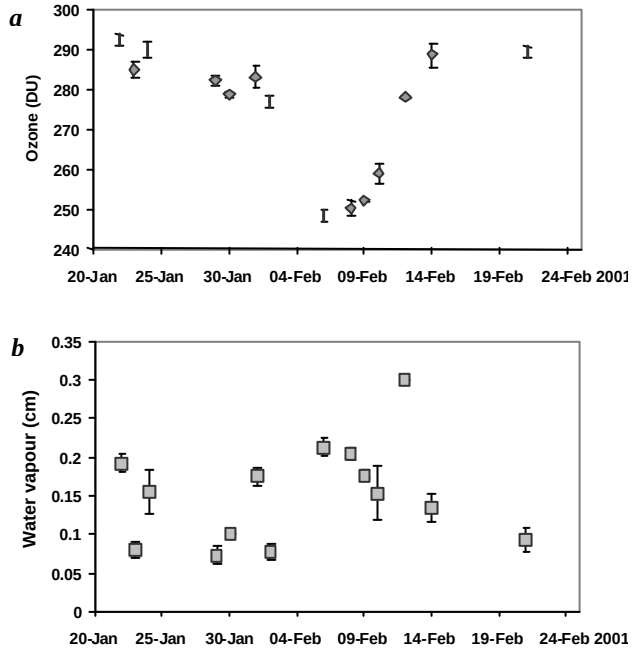

Figure 6. Daily mean columnar ozone (***a***) and total precipitable water-vapour (***b***) over Maitri, Antarctica. Vertical bar over datapoints represents standard deviation for that day.

vortex. Air back-trajectory analysis using HySPLIT[24,25] model shows that during the low ozone period, airmass came from low altitude and rose while reaching Maitri. Figure 7 shows the five days back-trajectory ending over Maitri on 5 February 2001. Figure 7 (top) shows the geographical location of the air parcel, whereas Figure 7 (bottom) shows its altitude variation with time. From the three air trajectories arriving at altitudes 10, 15 and 20 km, it is seen that the air at low altitude, which is ozone-deficit, is replacing the ozone-rich upper air and causing a local ozone minimum over the site. Figure 6*b* shows the daily mean value of the total precipitable water-vapour which is found to vary between 0.05 and 0.2 cm, with high values during the period when ozone minimum is observed. This further corroborates the earlier conclusion that the mixing between the lower and upper atmospheric air is responsible for the observed ozone minimum. In the case of water-vapour, its concentration is more at lower altitude and the vertical mixing from the airmass has resulted in an increase in the total columnar content during the above period.

Analysis of the spectral dependence of AOD provides a rough estimation on the aerosol size-distribution and chemical composition. Model AOD spectrum is calculated using OPAC (Optical Properties of Aerosol and Cloud) model[26] for the default values prescribed for Antarctica. OPAC describes ten aerosol components that are representative of different origins, with internally mixed chemical composition. The components could be externally mixed to get different aerosol types. Antarctic aerosol type in OPAC is same as that suggested by d'Almeida *et al.*[27], in which the major component is sulphate aerosol. In terms of mass, at 50% RH, sulphate contributes 91%, sea-salt accumulation 4.5% and mineral transported 4.5% to the total mass at the surface-level, which is about 2.2 μg/m^3. In the OPAC model, Antarctic AOD is calculated assuming an exponentially decreasing aerosol profile, with a scale height of 8 km. With this default aerosol profile and composition, the computed AOD is found to be high at lower wavelengths compared to the observed AOD. The mass concentration computed based on the OPAC parameters for particles of size less than 7.5 μm is lower compared to that measured by QCM, indicating that there is underestimation of the amount of bigger particles in the model. Also, the default Antarctic aerosol model could not explain the observed size-distribution. In order to have a better comparison and consistency between the measured data and the model, using information available on the chemical composition from earlier studies[20,28,29], we propose modifications to the Antarctic aerosol model prescribed in the OPAC model (see Table 2). The important change is to increase the concentration of the bigger particles while reducing the amount of the submicron (sulphate) particles. With this proposed modification, the computed AOD spectrum compares better with measurements (Figure 8). The dashed line represents the calculated AOD at 50% RH using the aerosol composition suggested in the OPAC model, while the continuous line represents the calculated AOD for the modified composition at 50% RH. With the new composition, the total mass for particles of size less than 7.5 μm becomes 5.6 μg m^{-3}, which is in better agreement with the measured mass value. Other aerosol properties like single scattering albedo and asymmetry factor are calculated using Mie theory, and are further used to calculate the aerosol direct radiative forcing.

Radiative transfer calculations are made using SBDART[15] for plane parallel atmosphere for short wave (SW; 0.25 to 2.5 μm) and long wave (LW; 2.5 to 40 μm) separately,

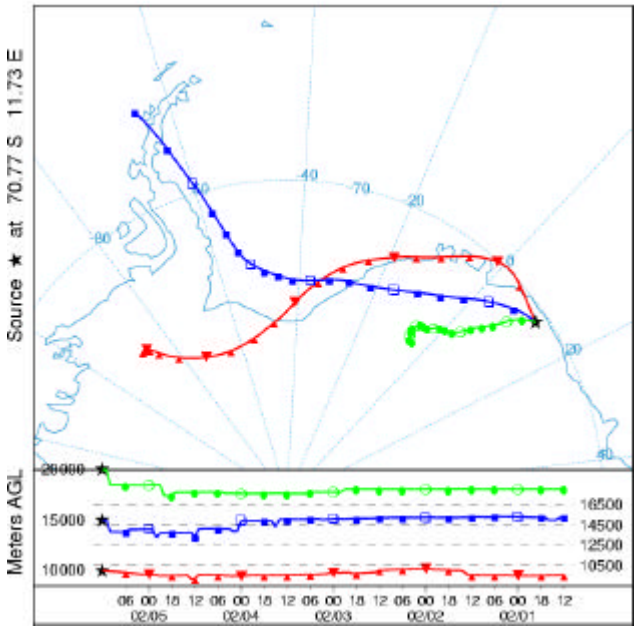

Figure 7. Five days back-trajectory on 5 February 2001 over Maitri, Antarctica. (Top) Geographical location of air parcel. (Bottom) Altitude variation of air parcel with time. Height is in metre above ground level.

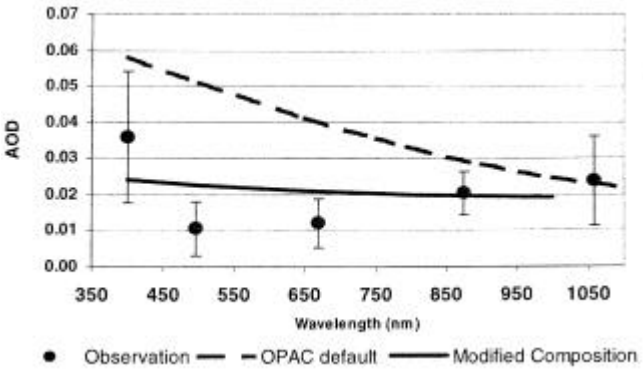

Figure 8. Comparison of the observed mean AOD spectrum over Maitri with that of the OPAC model computed at 50% relative humidity (broken line) and the modified composition (solid line).

Table 2. Parameters prescribed in the OPAC model for Antarctic aerosols and suggested modifications proposed in the present study to better explain the observed AOD spectrum and aerosol mass size-distribution

Component	Number density (cm^{-3})		r^*_{mod} (μm)	s	r^* (g/m^3)
	OPAC model	Suggested modification			
Sea-salt accumulation mode	0.047	–	0.336	2.03	1.29
Sea-salt coarse mode	–	0.015	2.82	2.03	1.29
Mineral transported	0.0053	0.1	0.5	2.2	2.6
Sulphate	42.9	0.05	0.0983	2.03	1.25

r_{mod} and s are respectively, mod radius and width parameter for log normal size-distribution.
s is density of aerosol particles.
*At 50% RH.

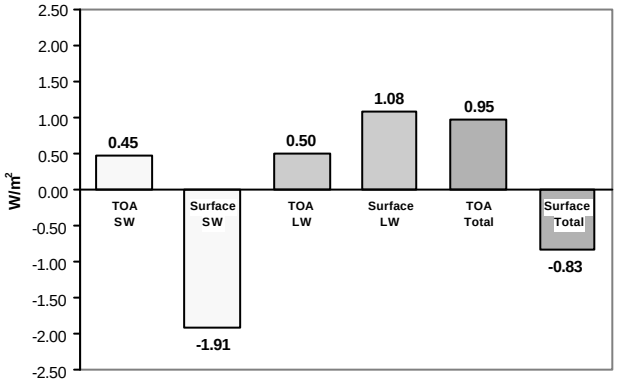

Figure 9. Diurnally averaged mean aerosol direct radiative forcing over Maitri, Antarctica for the observation period.

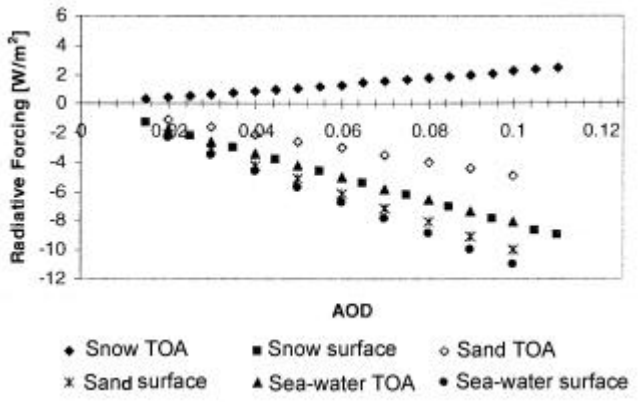

Figure 10. Variation in computed aerosol radiative forcing for the same aerosol composition and amount but for different surface types with varying surface albedo.

with and without aerosol. Long-wave calculations are carried out till 40 μm, as the solar energy above 40 μm is negligible. Hence the effect of aerosol in the excluded range could be neglected. Wavelength resolution used in the shorter wavelength range is 10 nm, while for longer wavelengths it is increased to the maximum resolution available in the model, i.e. 20 cm^{-1}. Atmospheric profile is constructed for February monthly mean conditions from FNL data for the lower atmosphere and merged with the summer sub arctic atmospheric profile. Default vertical profile from SBDART (Ricchiazzi *et al.*[15] and reference therein) is used for aerosols. Calculations of irradiance at the surface and the top of the atmosphere (TOA; at 100 km in this case) are done at 15 min interval for 24 h period, with and without aerosol. The aerosol radiative forcing is taken as the difference between the two estimates.

The computed 24 h average aerosol radiative forcing at the surface and TOA for SW and LW is shown in Figure 9. The forcing is positive at TOA for both SW and LW, but at the surface it is negative for SW and positive for LW. The net forcing is 0.95 W/m^2 at TOA and –0.83 W/m^2 at the surface, with absorption of 1.78 W/m^2 within the atmosphere. Positive radiative forcing at TOA over Maitri is due to high surface albedo, typical of the polar region. In comparison to regions of high anthropogenic activity, the observed aerosol radiative forcing over Antarctica is low. Jayaraman[30] has reported TOA SW aerosol forcing of about –6.9 W/m^2 over coastal India, –4.7 W/m^2 over the Arabian Sea and –1.45 W/m^2 over the tropical Indian Ocean. Satheesh[31] has found –7 W/m^2 in SW range and –4 W/m^2 total aerosol forcing over the Bay of Bengal. Higgnet *et al.*[32] have found –9 W/m^2 over the Atlantic Ocean.

In order to study the effect of surface albedo on TOA radiative forcing, the model computations are repeated for sand and sea-water surfaces, keeping the aerosol characteristics and amount the same as that found over Maitri (Figure 10). For unit AOD change, the TOA SW forcing will change by 22.5 W/m^2, –43.9 W/m^2 and –72.9 W/m^2 for snow, sand and sea-water types of surfaces respectively. The observed large change in the radiative forcing, from a high-reflective snow surface to low-reflective water surface can be understood, as explained by Harshvardhan[33] that the presence of aerosol over bright sur-

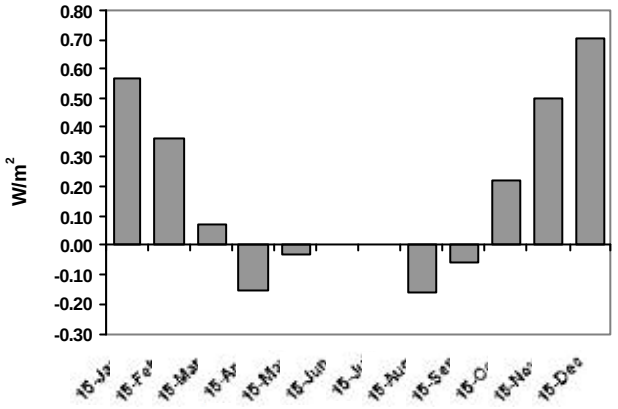

Figure 11. Annual variation in computed SW aerosol radiative forcing due to varying sun–earth geometry for a constant AOD spectrum.

faces has an overall effect of reducing the surface albedo, while over dark surfaces it has an overall effect of enhancing the albedo. Another interesting difference in aerosol direct radiative forcing over high-latitude regions such as Antarctica arises due to the sun–earth geometry. Over Antarctica, sunshine duration varies significantly from season to season and hence the SW aerosol radiative forcing. The computed variation in aerosol radiative forcing that arises due to varying sun–earth geometry is shown in Figure 11 for the 15th of each month, while the AOD is kept constant. SW radiative forcing by aerosol varies from a positive value of 0.7 in December to –0.15 in April and August, and it becomes zero for no sunshine days during June and July.

Conclusion

AOD over Antarctica is low, with the average value lying between 0.01 and 0.1 for all wavelengths during the observation period from January to February 2001. This is lower than the value obtained earlier over clean oceanic regions like the southern Indian Ocean. Surface-level ambient aerosol mass concentration is also low with an average value of 9.14 $\mu g/m^3$, which when corrected for the humidity (dry mass) becomes 6.97 $\mu g/m^3$. Coarse-mode particles are found to contribute about 63% to the total mass. The dominance of coarse-mode particles is also reflected in the obtained AOD spectrum, which is more or less flat. Calculations of aerosol radiative forcing show that though the optical depth values are low, they contribute to a net positive forcing of about 0.95 W/m^2 because of the high surface reflectance. Model computations repeated for the same aerosol amount but for different surface types reveal that for an unit AOD change, the TOA SW forcing values are +22.5 W/m^2, –43.9 W/m^2 and –72.9 W/m^2 respectively, for snow, sand and sea-water types of surfaces. Another interesting observation is that because of the strongly varying sun–earth geometry over the polar region, the radiative forcing exhibits strong seasonal dependence, varying from a positive value of 0.7 in December to –0.15 in April, and becomes zero during no sunshine days in June and July.

1. Ramanathan, V. *et al.*, Indian Ocean Experiment: An integrated analysis of the climate forcing and effects of the great Indo-Asian haze. *J. Geophys. Res.*, 2001, **106**, 28371–28398.
2. Russell, P. B., Hobbs, P. V. and Stowe, L. L., Aerosol properties and radiative effects in the United States East Coast haze plume: An overview of the Tropospheric Aerosol Radiative Forcing Observational Experiment (TARFOX). *J. Geophys. Res.*, 1999, **104**, 2213–2222.
3. Bates, T. S., Huebert, B. J., Gras, J. L., Griffiths, F. B. and Durkee, P. A., International Global Atmospheric Chemistry (IGAC) Project's First Aerosol Characterization Experiment (ACE 1): Overview. *J. Geophys. Res.*, 1998, **103**, 16297–16318.
4. Jayaraman, A., Lubin, D., Ramachandran, S., Ramanathan, V., Woodbridge, E., Collins, W. D. and Zalpuri, K. S., Direct observations of aerosol radiative forcing over the tropical Indian Ocean during the January–February 1996 pre-INDOEX cruise. *J. Geophys. Res.*, 1998, **103**, 13827–13836.
5. Satheesh, S. K. and Ramanathan, V., Large difference in tropical aerosol forcing at the top of the atmosphere and earth's surface. *Nature*, 2000, **405**, 60–63.
6. Rajeev, K. and Ramanathan, V., Direct observations of clear-sky aerosol radiative forcing from space during the Indian Ocean Experiment. *J. Geophys. Res.*, 2001, **106**, 17221–17236.
7. Podgorny, I. A., Conant, W. C., Ramanathan, V. and Satheesh, S. K., Aerosol modulation of the surface and atmospheric solar heating over the tropical Indian ocean. *Tellus*, 2000, **52**, 947–958.
8. Shaw, G. E., Atmospheric turbidity in the polar regions. *J. Appl. Meteorol.*, 1982, **21**, 1080–1088.
9. Herber, A., Thomason, L. W., Radionov, V. F. and Leiterer, U., Comparison of trends in the tropospheric and stratospheric aerosol optical depths in the Antarctic. *J. Geophys. Res.*, 1993, **98**, 18441–18447.
10. Herber, A., Thomason, L. W., Dethloff, K., Viterbo, P., Radionov, V. F. and Leiterer, U., Volcanic perturbation of the atmosphere in both polar regions: 1991–1994. *J. Geophys. Res.*, 1996, **101**, 3921–3928.
11. Sharma, S. D. and Sharma, M. C., Erythemal and aerosol studies at Maitri, Antarctica during austral spring of 1995. *Indian J. Phys.*, 1999, **73B**, 463–472.
12. Shaw, G. E., Sun photometry. *Bull. Am. Meteorol. Soc.*, 1983, **64**, 4–10.
13. Young, A. T., Air mass and refraction. *Appl. Opt.*, 1994, **33**, 1108–1110.
14. Nicolet, M., On the molecular scattering in the terrestrial atmosphere: An empirical formula for its calculation in the homosphere. *Planet. Space Sci.*, 1984, **32**, 1467–1468.
15. Ricchiazzi, P., Yang, S., Gautier, C. and Sowle, D., SBDART: A research and teaching software tool for plane-parallel radiative transfer in the earth's atmosphere. *Bull. Am. Meteorol. Soc.*, 1998, **79**, 2101–2114.
16. Wallace, D. and Chuan, R., A cascade impaction instrument using quartz crystal microbalance sensing elements for 'real-time' particle size-distribution studies. 8th Materials Research Symposium on Methods and Standards for Environmental Measurement, 1976.
17. Morys, M., Mims III, F. M., Hagerup, S., Anderson, S. E., Baker, A., Kia, J. and Walkup, T., Design, calibration, and performance of Microtops II handheld ozone monitor and sun photometer. *J. Geophys. Res.*, 2001, **106**, 14573–14582.

18. Jayaraman, A., Satheesh, S. K., Mitra, A. P. and Ramanathan, V., Latitude gradient in aerosol properties across the inter tropical convergence zone: Results from the joint Indo–US study onboard *Sagar Kanya*. *Curr. Sci.*, 2001, **80**, 128–137.
19. Ramachandran, S. and Jayaraman, A., Pre-monsoon aerosol mass loadings and size-distributions over the Arabian Sea and the tropical Indian Ocean. *J. Geophys. Res.*, 2002, **107**, AAC1.1–1.21.
20. Mazzera, D. M., Lowenthal, D. H., Chow, J. C., Watson, J. G. and Grubisic, V., PM_{10} measurements at McMurdo Station, Antarctica, Atmos. *Environ*, 2001, **35**, 1891–1902.
21. Hall, J. S. and Wolff, E. W., Causes of seasonal and daily variations in aerosol sea-salt concentrations at a coastal Antarctic Station. *Atmos. Environ.*, 1998, **32**, 3669–3677.
22. Richardson, C., Phase relationships in sea ice as a function of temperature. *J. Glaciol.*, 1976, **17**, 507–519.
23. TOMS, Total Ozone Mapping Spectrometer data available at following website: http://toms.gsfc.nasa.gov/
24. Draxler, R. R. and Rolph, G. D., HYSPLIT (HYbrid Single-Particle Lagrangian Integrated Trajectory) model access via NOAA ARL READY website: http://www.arl.noaa.gov/ready/hysplit4.html. NOAA Air Resources Laboratory, Silver Spring, MD, 2003.
25. Rolph, G. D., Real-time Environmental Applications and Display sYstem (READY) website: http://www.arl.noaa.gov/ready/hysplit4.html. NOAA Air Resources Laboratory, Silver Spring, MD, 2003.
26. Hess, M., Koepke, P. and Schult, I., Optical properties of aerosols and clouds: The software package OPAC. *Bull. Am. Meteorol. Soc.*, 1998, **79**, 831–844.
27. d'Almeida, G. A., Koepke, P. and Shettle, E. P., *Atmospheric Aerosols: Global Climatology and Radiative Characteristics A*, Deepak Publishing, 1991, p. 561.
28. Wagenbach, D. *et al.*, Sea-salt aerosol in coastal Antarctic regions. *J. Geophys. Res.*, 1998, **103**, 10961–10974.
29. Kerminen, V., Teinila, K. and Hillamo, R., Chemistry of sea-salt particles in the summer Antarctic atmosphere. *Atmos. Environ.*, 2000, **34**, 2817–2825.
30. Jayaraman, A., Aerosol radiative forcing over the tropical Indian Ocean. *Proc. Indian Natl. Sci. Acad.*, 2001, **67**, 385–394.
31. Satheesh, S. K., Radiative forcing by aerosols over Bay of Bengal region. *Geophys. Res. Lett.*, 2002, **29**, 40.1–40.4.
32. Hignett, P., Taylor, J. P., Francis, P. N. and Glew, M. D., Comparison of observed and modeled direct aerosol forcing during TARFOX. *J. Geophys. Res.*, 1999, **104**, 2279–2287.
33. Harshvardhan, Aerosol-climate interactions. *Aerosol–Cloud–Climate Interactions* (ed. Hobbs, P. V.), Academic Press, 1993, p. 233.

ACKNOWLEDGEMENTS. The experiment was funded by the ISRO-Geosphere Biosphere Programme of the Department of Space, Government of India. We thank Director, PRL, the National Centre for Antarctic and Oceanographic Research, Goa and the Department of Ocean Development for selecting one of the authors (H.G.) to participate in the XX Indian Antarctic Expedition. We acknowledge the NOAA Air Resources Laboratory for the provision of the HySPLIT transport and dispersion model and READY website (http: //www.arl.noaa.gov/ready.html) used in this publication. NCEP reanalysis data were provided by the NOAA–CIRES Climate Diagnostic Center, Boulder, Colorado, USA through their web site http://www.cdc.noaa.gov/. Radiative Transfer calculations were carried out using IBM-RS6000-SP machine at PRL.

Received 28 July 2003; accepted 9 September 2003